

Performance Study of a Solid Fuel-Pulsed Electric Microthruster

ALBERT SOLBES*
MIT, Cambridge, Mass.

AND
ROBERT J. VONDRA†
MIT, Lincoln Laboratory, Lexington, Mass.

A study of the over-all operating characteristics of a parallel rail solid fuel-pulsed microthruster is presented. Specifically, the effect of several electrical circuit parameters (capacitance, inductance, resistance) on performance (impulse bit, specific impulse, efficiency) has been investigated. The experimental results, combined with a simple model for the mass ablation and the acceleration mechanisms, provide useful correlations between thruster geometrical and electrical circuit parameters and its performance. These results should be useful in improving the performance and optimizing the design of a thruster for a given mission.

Introduction

SLID fuel electric microthrusters, where the propellant (Teflon) is ablated, ionized and accelerated by means of an intense (several ka) electric discharge of short duration (a few μ seconds), offer definite advantages over other conventional thrusters for missions where emphasis is placed on thrust accuracy, simplicity (reliability) and long lifetime. Such thrusters have, for example, been flown and operated with success by Lincoln Lab.,¹ on board the LES-6 experimental communication satellite, for East-West stationkeeping. However, thrusters of this type suffer, in spite of recent improvements, from the low value of their specific thrust (~ 3 to $4 \mu\text{lb/w}$) and efficiency ($\leq 10\%$). Consequently, a research program was initiated in 1968 by Lincoln Lab., aimed at improving the thruster's performance. Part of the efforts were concentrated on the study of the electrical discharge and plasma characteristics. The results obtained^{2,3} have shed some light on the nature of the acceleration mechanism and helped identify the main losses. Simultaneously, a program aimed at the determination of the over-all operating characteristics of such thrusters was undertaken. The effect of changes, in various electric parameters, on thruster performance was systematically investigated. We propose to present hereafter some of the experimental results obtained to date. These, when combined with a simple model for the thruster, provide useful correlations between geometrical and electrical circuit parameters and thrust performance.

Thruster Description and Equivalent Electric Circuit

Detailed descriptions of the thruster can be found in the literature.^{2,3} We will simply recall here the main features. The thruster under investigation consists essentially of a storage capacitor, a Teflon fuel block, a triggering circuit and a thrust chamber. Energy is stored in the capacitor of a few microfarads (a few joules under typically 1000–2000 v). By means of a 6-v trigger pulse, a low energy discharge (< 0.5 joules) is initiated in the vicinity of the Teflon surface forming the backwall of the thrust chamber. This, in turn, initiates a current flow between the electrodes, from the main storage

capacitor. The ensuing discharge ablates, ionizes and accelerates the plasma, thus providing the desired thrust (Fig. 1). A negator spring feeds the Teflon fuel as it is ablated.

A simple equivalent circuit for the thrusters is shown in Fig. 2, where the total resistance and inductance (R and L) include the capacitor (R_c and L_c), the leads and electrodes (R_e and L_e), as well as the plasma (R_p and L_p). The above lumped description of the circuit poses no special difficulty except for the plasma parameters. In the interelectrode spacing the electromagnetic field satisfies Maxwell's equations which can be written in the MHD approximation.

$$\nabla \times \mathbf{E} = -\partial \mathbf{B} / \partial t \quad (1)$$

$$\nabla \times \mathbf{B} = \mu_0 \mathbf{J} \quad (2)$$

where \mathbf{E} , \mathbf{B} and \mathbf{J} are, respectively, the electric field, magnetic induction and current density vectors. An electric field potential ϕ and a vector potential \mathbf{A} can be defined such that

$$\mathbf{B} = \nabla \times \mathbf{A} \quad (3)$$

$$\mathbf{E} = -\nabla \phi - (\partial \mathbf{A} / \partial t) \quad (4)$$

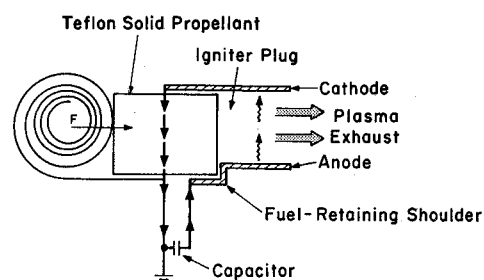


Fig. 1 Solid fuel microthruster (schematic).

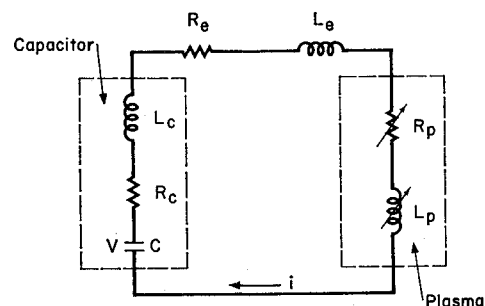


Fig. 2 Thruster's equivalent electrical circuit.

Presented as Paper 72-458 at the AIAA 9th Electric Propulsion Conference, Bethesda, Md., April 17–19, 1972; submitted May 30, 1972; revision received January 10, 1973. This work was sponsored by the Department of the Air Force.

Index category: Electric and Advanced Space Propulsion.

* Associate Professor of Aeronautics and Astronautics. Member AIAA.

† Staff Member, Space Communications Division. Member AIAA.

Furthermore, relating the current density to the electric field and magnetic field vectors by Ohm's law leads to

$$\mathbf{J} = \sigma[\mathbf{E} + \mathbf{U} \times \mathbf{B}] \quad (5)$$

where for simplicity the Hall effect has been neglected, σ being the scalar conductivity of the plasma, and \mathbf{U} the fluid velocity. Combination of Eqs. (3-5) yields

$$-\nabla\phi = (\mathbf{J}/\sigma) - \mathbf{U} \times \mathbf{B} + (\partial\mathbf{A}/\partial t) \quad (6)$$

In the right-hand side of the preceding equation, the successive terms correspond respectively to a resistive voltage drop, a back emf due to the motion of the gas and an inductive term. The first two terms (averaged over the plasma volume) have been combined in our definition of the plasma resistance R_p . Dotting Eq. (6) by the current density vector and integrating over the plasma volume yields

$$\begin{aligned} iV_p &= - \int_V \phi \mathbf{J} \cdot d\mathbf{S} \\ &= \int_V \frac{J^2}{\sigma} dV + \int_V \mathbf{U} \cdot (\mathbf{J} \times \mathbf{B}) dV + \int_V \mathbf{J} \cdot \frac{\partial \mathbf{A}}{\partial t} dV \end{aligned} \quad (7)$$

where the power into the plasma, product of the circuit current i by the voltage difference between electrode V_p , appears as the sum of a joule heating term, the power due to Lorentz forces and an inductive term.

Experimental Procedure and Results

For the experiments to be described hereafter, a fixed geometry parallel rail thruster was used. The electrodes, 3 cm apart, were 1 cm wide and 0.6 cm long. The fuel was Teflon. The following electric parameters were varied: C from 0.66 to 6 μF , V from 500 to 2000 v, R_e from 0 to 0.8 Ω , L_e from 50 to 650 nH. For each set of values in the preceding parameters, thrust and fuel consumption were measured with the aid of a simple thrust stand and a precision mass balance. The thrust stand consists essentially of a pendulum on which the thruster is fixed. The thruster is fired in synchronism with the motion of the pendulum. Recording the changes in amplitude allows a determination of the average value of impulse per shot. These measurements, together with the knowledge of the electrical energy stored, allow the determination of the specific impulse (electrode erosion is negligible) and thruster efficiency.

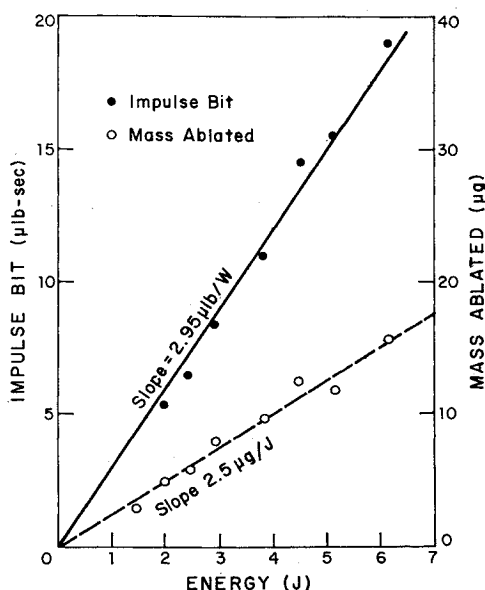


Fig. 3 Impulse bit vs energy ($C = 4 \mu\text{F}$), mass ablated vs energy ($C = 4 \mu\text{F}$).

Photographs of the voltage waveform were also taken during the discharge. For the damped oscillatory waveforms usually observed, the average circuit inductance L and resistance R , can be determined.

Examination of the experimental results shows that for a fixed capacitance and electric configuration, the impulse bit, I , and the mass ablated per shot, m , are approximately proportional to the discharge energy E . This is illustrated in Fig. 3, where the impulse and mass ablated per shot have been plotted as a function of E for a 4 μF capacitance. Hence, it results that the specific impulse, I_{sp} , and efficiency are independent of the capacitor voltage in the range investigated. However, as R , L and C are changed, one observes in general changes in the impulse, mass ablated, specific impulse and efficiency. Figure 4 illustrates, as an example, the effect of changes in the circuit inductance on the specific impulse.

We propose hereafter, with the aid of the data gathered and of a simple model for the thruster, to develop semiempirical relationships which will correlate the thruster performance with its electrical and geometrical characteristics. Relationships for the fuel consumption and specific thrust will be established first, from which specific impulse and efficiency will automatically follow.

Specific Fuel Consumption

During a discharge, the exposed Teflon surface forming the backwall of the thrust chamber is subject to a heat flux from the adjoining plasma, thus leading to fuel ablation. We will assume the ablation rate to be energy limited and postulate that "the mass ablated per shot is proportional to the energy dissipated electrically in the vicinity of the Teflon surface," without specifying, however, the nature of the energy transport mechanism. More specifically, we write that the mass ablated, m , times the latent heat of vaporization, λ , of the fuel, is equal to the energy dissipated in a layer of conductivity σ_0 and thickness ϵ located at the thrust chamber backwall. This leads to an expression of the form

$$m = (\sigma_0 \epsilon / \lambda) (d/h) [(R_p^2 + L_p^2 / LC) / R] E \quad (8)$$

where h is the distance between electrodes, d their width and an equivalent total circuit resistance is defined as

$$R = E / \int_0^\infty i^2 dt \quad (9)$$

i being the value of the instantaneous discharge current. In Eq. (8), $\sigma_0 \epsilon d / h$ has the dimensions of a conductance and is taken to be characteristic of a standing ablating arc which is in parallel with the plasma impedance. The existence of such a

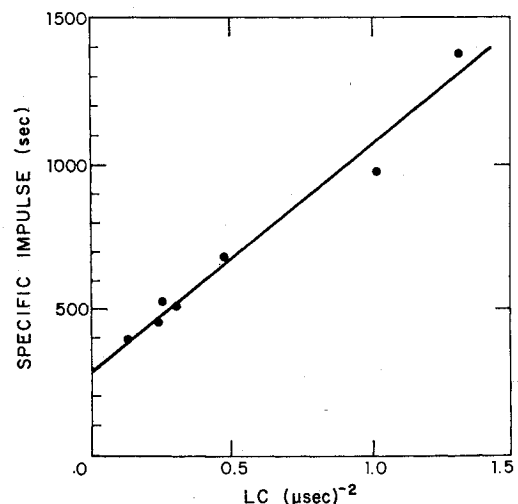


Fig. 4 Effect of circuit inductance on specific impulse ($C = 2 \mu\text{F}$).

standing arc has been confirmed by pictures of the discharge taken with an image converter camera.³ The product $\sigma_0 \epsilon$ can be thought of as a surface property whose value is approximately constant and is to be determined experimentally. For all the available experimental points the mass ablated per shot was plotted as a function of the electrical parameters in the way suggested by Eq. (8). The results are presented in Fig. 5, which illustrates the existence of a very good correlation as proposed. The best fit for the data is obtained for a value of $\sigma_0 \epsilon$ equal to 0.275 mho. This would lead, for an estimated value of $\sigma_0 \approx 3000$ mho/m ($T_e \approx 1$ v), to an ablation layer thickness of the order of 0.1 mm. For fixed values of the electric circuit parameters, Eq. (8) predicts the proportionality between mass ablated and discharge energy. A more severe test of the proposed correlation can be made by considering

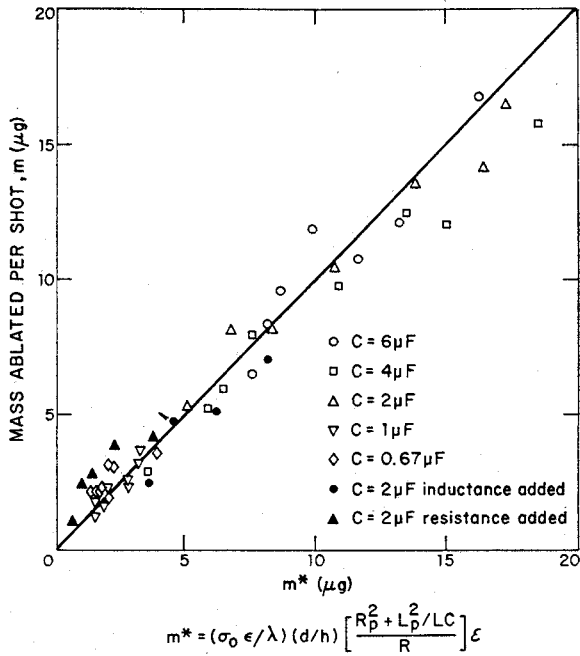


Fig. 5 Ablated mass per shot correlation ($\sigma_0 \epsilon = 0.275$ mho).

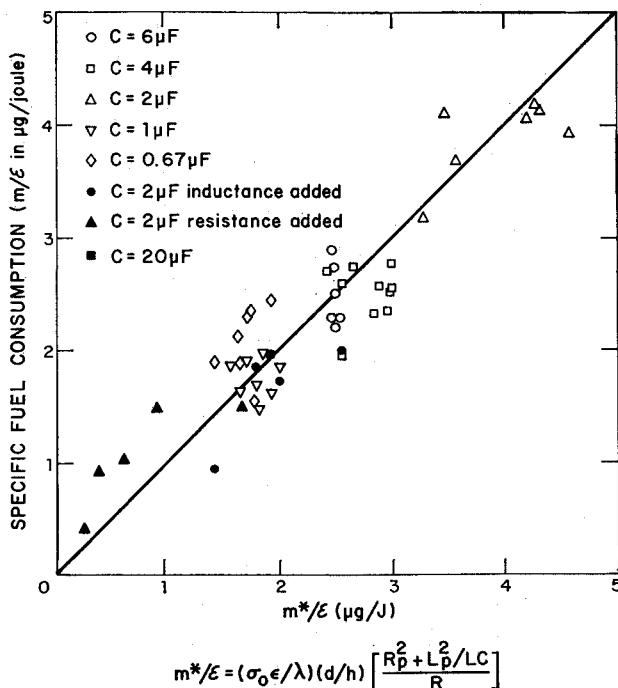


Fig. 6 Specific fuel consumption correlation ($\sigma_0 \epsilon = 0.275$).

the specific fuel consumption dependence (hence, removing the energy dependence) on the circuit parameters. This was done and the results are presented in Fig. 6. The correlation is still seen to be quite good, most of the scatter (15–20%) being attributed mainly to uncertainties in the determination of the circuit parameters. From Eq. (8), it can be noted that increases in circuit resistance, inductance and capacitance all lead to a reduction in the specific fuel consumption.

Impulse Bit

The momentum equation for an infinitesimal plasma volume can be written in a differential form

$$\frac{\partial \rho \mathbf{U}}{\partial t} + \nabla \cdot [\rho \mathbf{U} \mathbf{U} + \mathbf{P}] = \mathbf{J} \times \mathbf{B} = -\nabla \left(\frac{B^2}{2\mu_0} \right) + \frac{\mathbf{B}}{\mu_0} \cdot \nabla \mathbf{B} \quad (10)$$

where \mathbf{P} is the pressure tensor and ρ the fluid density. The preceding equation can be integrated over a volume bounded by the thrust chamber walls and extending to large distances in the exhaust direction. The gradient terms lead to surface integrals.

$$(d\mathbf{M}/dt) + \int_S [\rho \mathbf{V} \mathbf{V} + \mathbf{P} + (B^2/2\mu_0)] \cdot d\mathbf{S} = \int_S (\mathbf{B}/\mu_0)(\mathbf{B} \cdot d\mathbf{S})$$

where \mathbf{M} is the momentum of the fluid enclosed at time t in the control volume. Integrating the preceding equation over time $t = 0$ to infinity and neglecting nondiagonal (viscous) terms in the pressure tensor, yields, noticing that \mathbf{M} is zero at both limits,

$$I = mU_0 + A_0 \int_0^\infty \left(n_0 k T_0 + \frac{B_0^2}{2\mu_0} \right) dt$$

where we have considered the momentum component along the thrust axis. The integrated mass flux has been identified with the mass ablated and the subscript zero refers to conditions at the thrust chamber backwall (Teflon surface) of area A_0 . U_0 is the fluid velocity at the surface, n_0 being the particle number density and T_0 their temperature (the electronic pressure is assumed negligible at the wall). The thruster has been assumed to exhaust in vacuum. The above equation suggests an expression for the impulse of the form

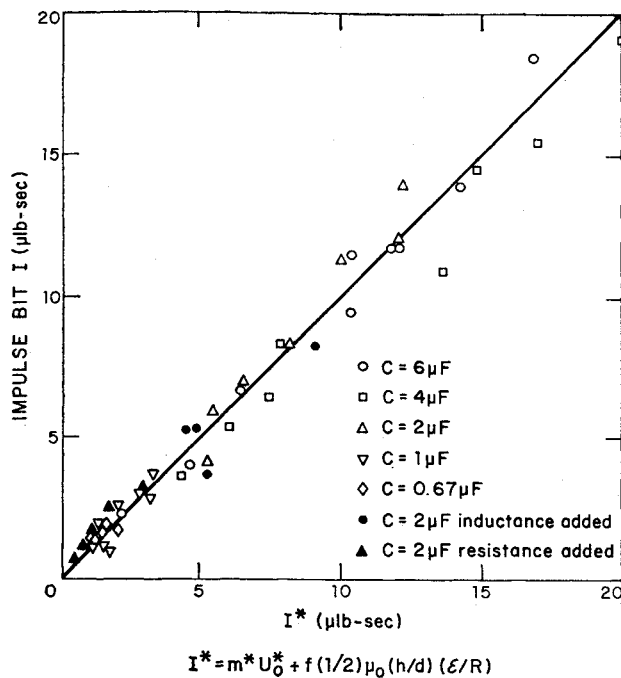
$$I = mU_0^* + \frac{1}{2} f \mu_0 (h/d)(E/R) \quad (11)$$

The first term in the right-hand side of Eq. (11) is proportional to mass and represents the gas dynamic contribution to the thrust, U_0^* being an effective velocity which accounts for the initial velocity and the pressure term. The second term represents the electromagnetic contribution. The magnetic pressure has been evaluated as a function of the current in a one-dimensional case (electrode width \gg electrode distance) and the factor $f \leq 1$ corrects for fringing and other three-dimensional effects. Combining Eqs. (8) and (11) leads to:

$$I = [U_0^*(\sigma_0 \epsilon / \lambda)(d/h)(R_p^2 + L_p^2/LC) + \frac{1}{2} f \mu_0 (h/d)](E/R) \quad (12)$$

This equation predicts a linear dependence of the impulse bit on the energy for fixed electric circuit parameters as is observed experimentally. A plot of the thrust measurements for all experimental points as a function of the preceding combination of the thruster parameters is shown in Fig. 7. The proposed correlation is seen to be verified quite accurately. The best fit is obtained for $U_0^* = 1225$ m/sec and $f = 0.253$. A more severe test can be performed by removing the energy dependence. This is done in Fig. 8 where the specific thrust is seen to satisfy the proposed correlation. In the range of parameters investigated, the gas dynamic and electromagnetic contribution to the thrust were of comparable magnitudes. From Eq. (12) it is seen again that increasing R , L or C will decrease the thrust. Here, however, increasing the circuit resistance has the most damaging effect.

The proposed model in which the contribution to thrust

Fig. 7 Impulse bit correlation ($U_0^* = 1225$ m/sec, $f = 0.253$).

from electromagnetic forces is independent of the mass ablated is consistent with the results of exhaust diagnostics³ which indicate that a small fraction of the fuel (<10%) is highly ionized and ejected at high velocities (20–40 km/sec). This also explains the possibility of achieving high values of the specific impulse by fuel "starvation."⁴

From the preceding expressions for the thrust and mass ablated, we can immediately derive expressions of the specific impulse and efficiency

$$I_{sp} = I/mg \quad (13)$$

$$\eta = \frac{1}{2} (I \times I_{sp} / E) g \quad (14)$$

Because of the linear dependence of the mass ablated and of the impulse bit on energy, both the specific impulse and

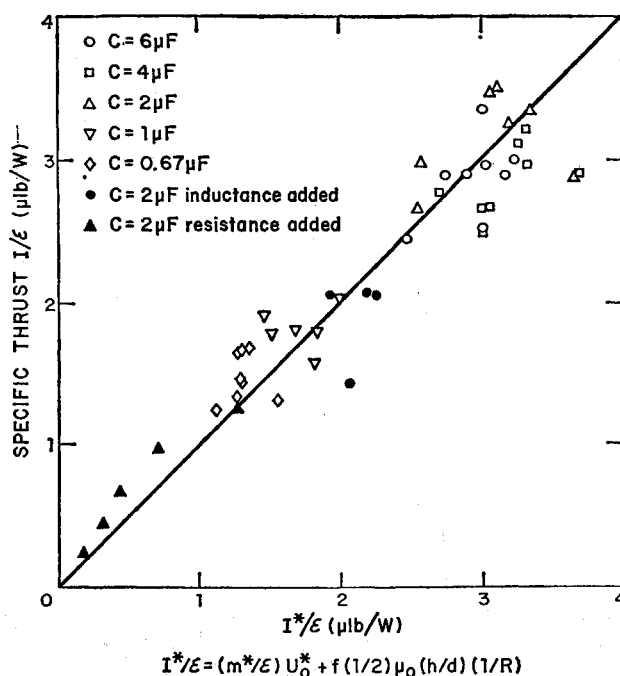
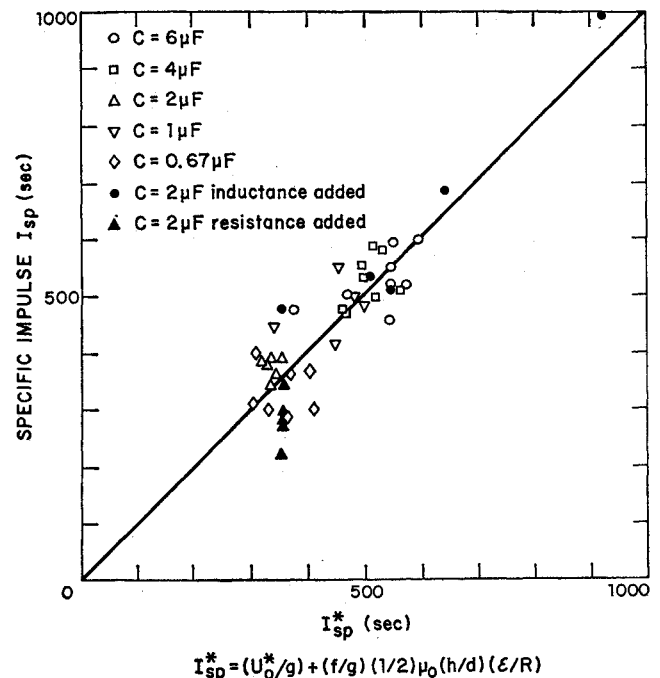
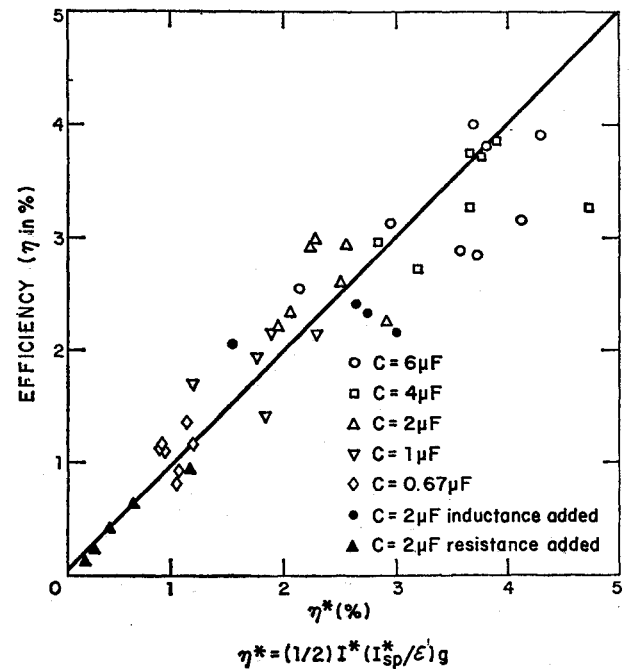
Fig. 8 Specific thrust correlation ($U_0^* = 1225$ m/sec, $f = 0.253$).Fig. 9 Specific impulse correlation ($U_0^* = 1225$ m/sec, $f = 0.253$).

Fig. 10 Efficiency correlation.

efficiency will be insensitive to changes in E . The specific impulse will also be insensitive to the total circuit resistance and will depend principally on L and C . The correlation obtained from the above relationships for the I_{sp} is shown in Fig. 9. Increasing the circuit capacitance and inductance both result in increases in specific impulse. Similarly, the efficiency is found to depend essentially on the circuit resistance. The correlation is shown in Fig. 10 and is found here again to be quite satisfactory in the range of parameters investigated.

Conclusions

The aforementioned results confirm the validity of the model hypothesized for the ablation and acceleration processes

in solid fuel microthrusters of the type investigated. They also allow to identify methods of improving the performance of such thrusters and optimizing a thruster for a given mission. High-specific impulse (~ 1500 sec) operation can be readily achieved by increasing the circuit inductance. High-specific thrusts require low inductances, capacitances and resistances. This seems more difficult to realize and accordingly present parallel rail thrusters rarely exceed specific thrusts of the order of $4 \mu\text{lb/w}$. The above analysis, however, suggests the possibility of increasing specific thrust by increasing the fuel area and, hence, mass ablation. Recent experiments have led to values of specific thrust three or four times larger than presently reported.⁴

References

- ¹ Guman, W. J. and Nathanson, D. M., "Pulsed Plasma Microthruster Propulsion System for Synchronous Orbit Satellite," *Journal of Spacecraft and Rockets*, Vol. 7, No. 4, April 1970, p. 409.
- ² Vondra, R., Thomassen, K., and Solbes, A., "Analysis of Solid Teflon Pulsed Plasma Thruster," *Journal of Spacecraft and Rockets*, Vol. 7, No. 12, Dec. 1970, pp. 1402-1406.
- ³ Vondra, R., Thomassen, K., and Solbes, A., "A Pulsed Electric Thruster for Satellite Control," *Proceedings of the IEEE*, Vol. 59, No. 2, Feb. 1971, p. 271.
- ⁴ Vondra, R. J. and Thomassen, K. I., "Performance Improvements in Solid Fuel Microthrusters," *Journal of Spacecraft and Rockets*, Vol. 9, No. 10, Oct. 1972, pp. 738-742.